

Impact of binding to the Multidrug Resistance Regulator protein LmrR on the photo-physics and -chemistry of photosensitizers

Sara H. Mejías,^{*a} Gerard Roelfes,^a and Wesley R. Browne^{*,a}

Electronic Supporting information

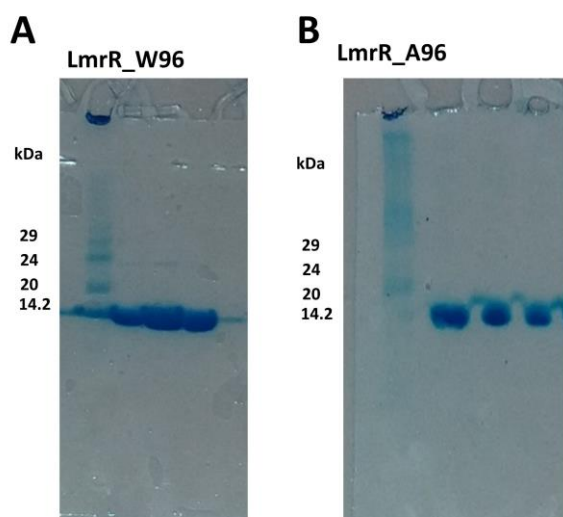


Figure S1. SDS-page gels of purified LmrR mutants. Left, LmrR_W96, and right, LmrR_A96.

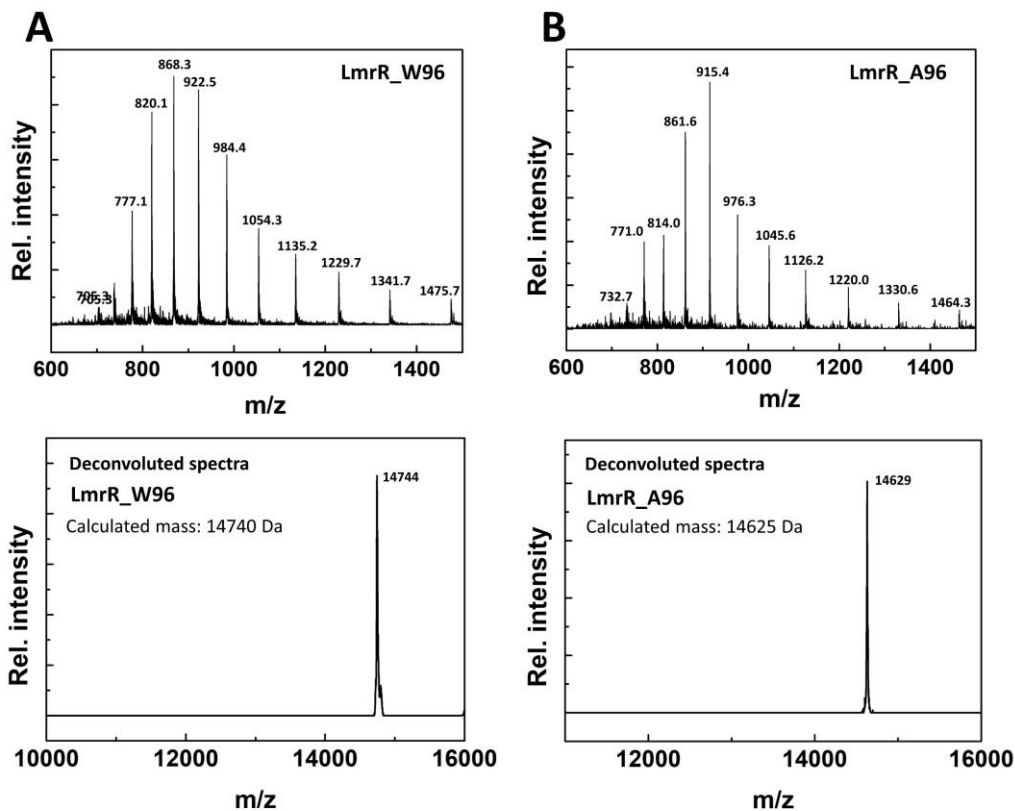


Figure S2. Electrospray ionization (ESI) mass spectra LmrR_W96 and LmrR_A96.

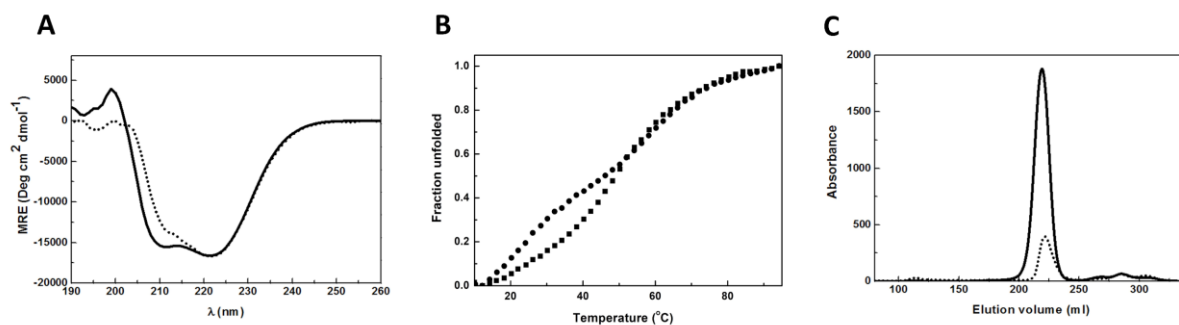


Figure S3. (a) Circular dichroism spectrum, (b) thermal denaturation and (c) size exclusion chromatography of LmrR_W96 (solid lines and squares) and LmrR_W96A (dotted lines).

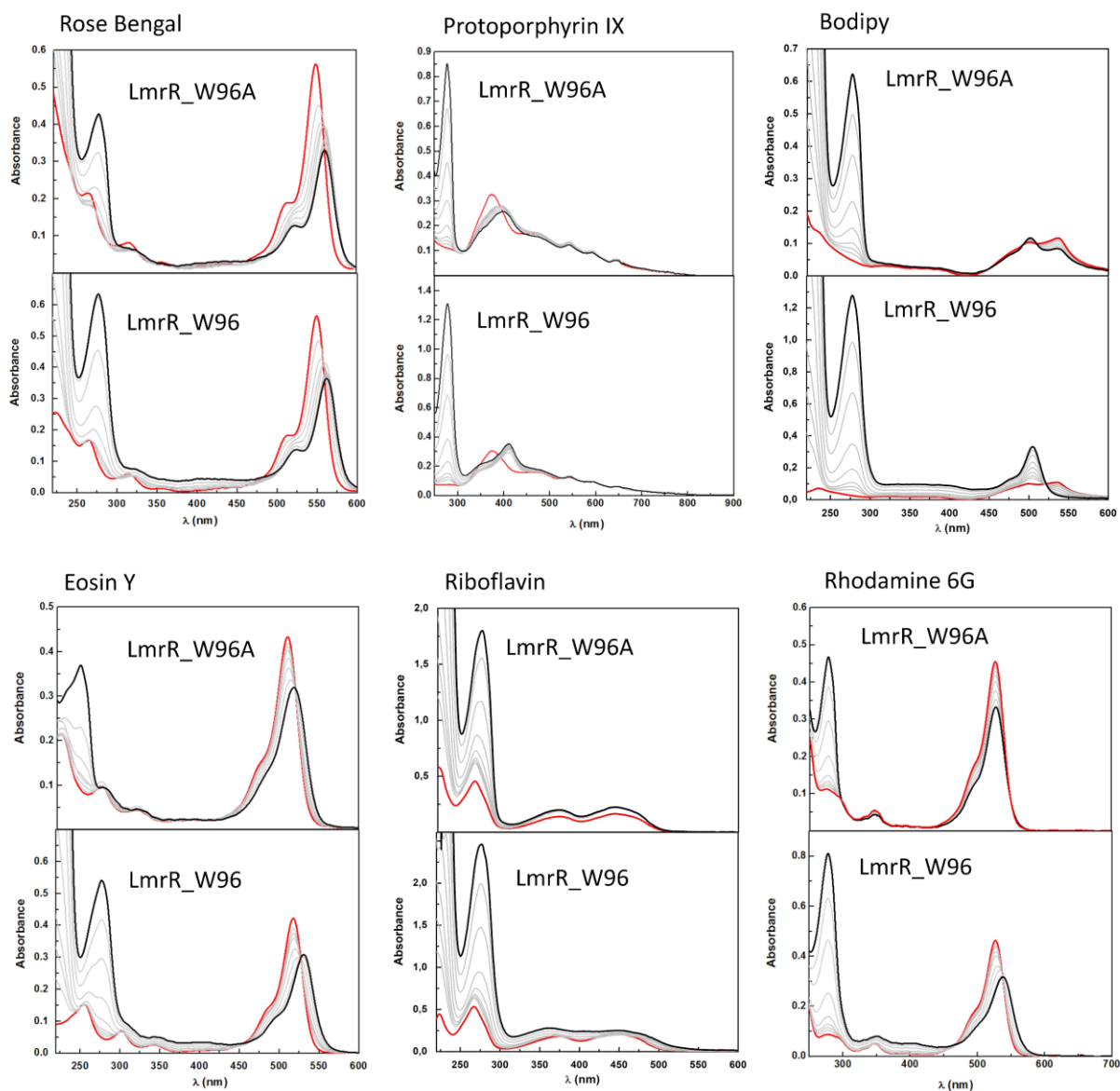
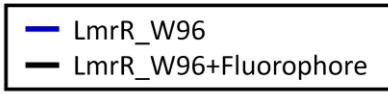
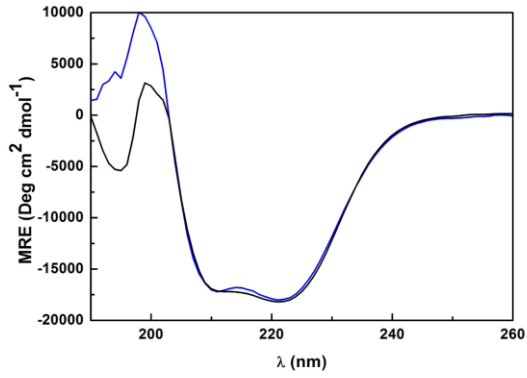
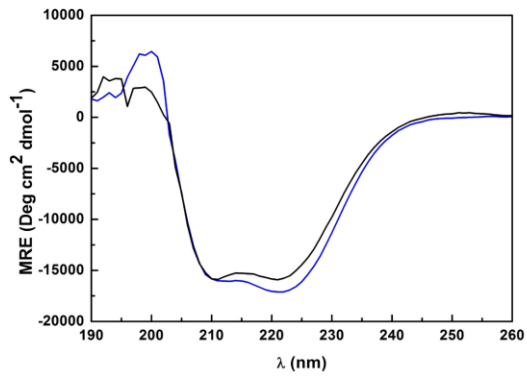
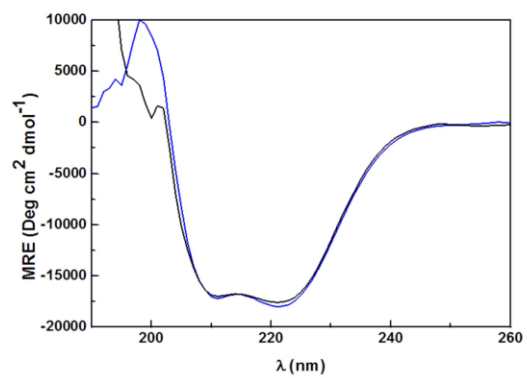
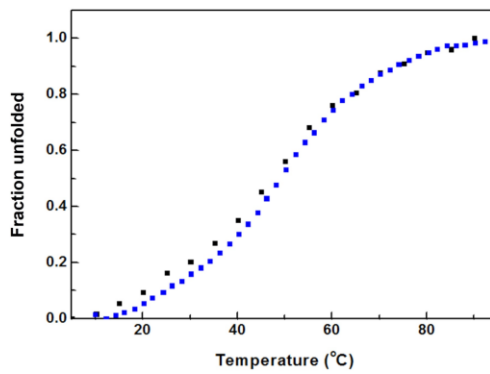
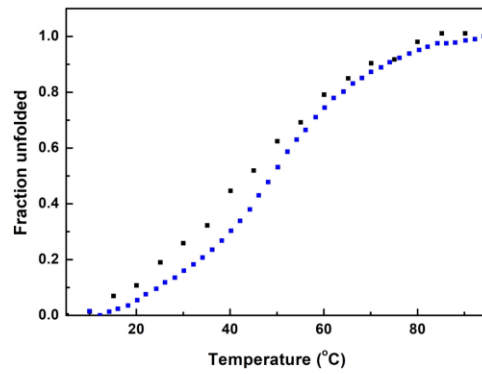
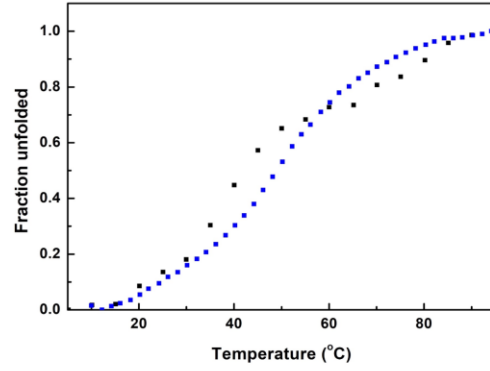


Figure S4. UV-vis absorbance spectra of dyes (at constant concentration) with increasing concentration from 0.1 equiv. (red line) to 10 equiv. (black line) of LmrR_W96A or LmrR_W96.

A**LmrR_W96 + RB****LmrR_W96 + PpIX****LmrR_W96 + Bodipy****B**

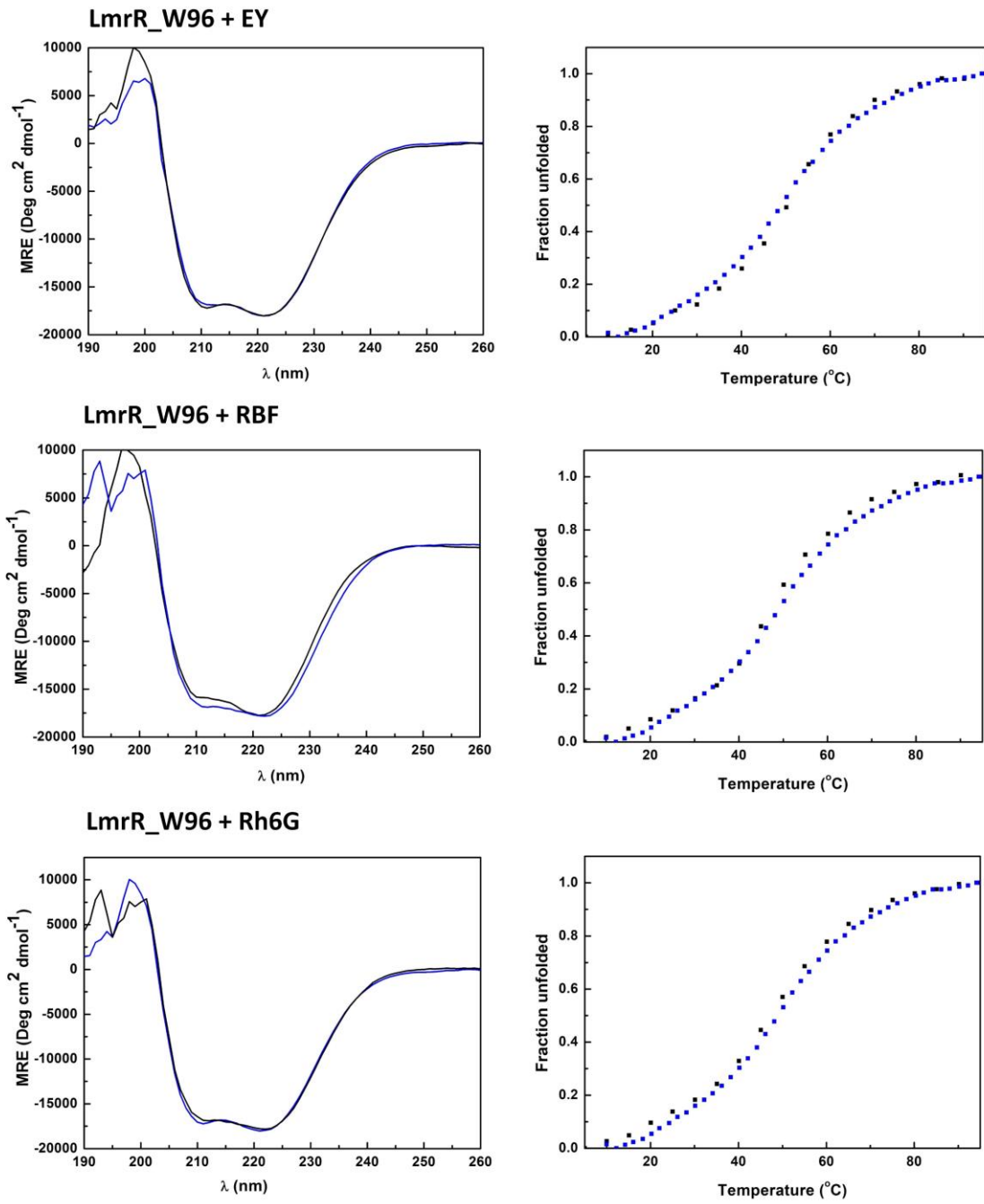


Figure S5. (a) Circular dichroism spectra and (b) thermal denaturation of LmrR_W96 (blue) and LmrR_W96 in the presence of the dyes (black).

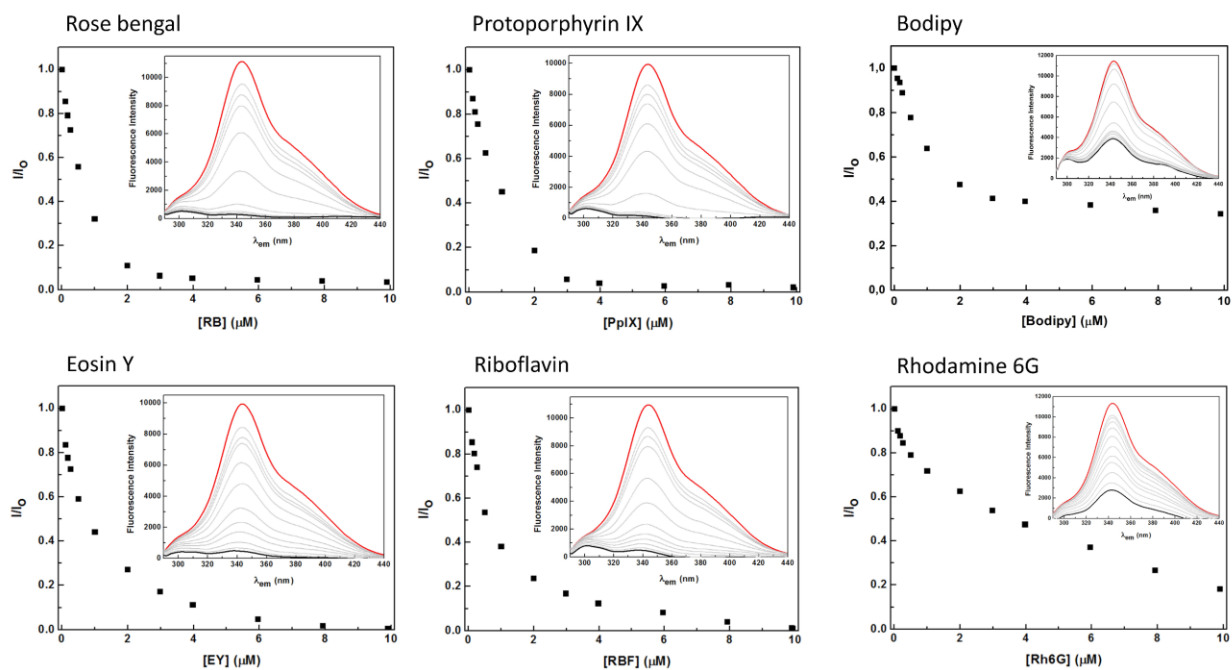
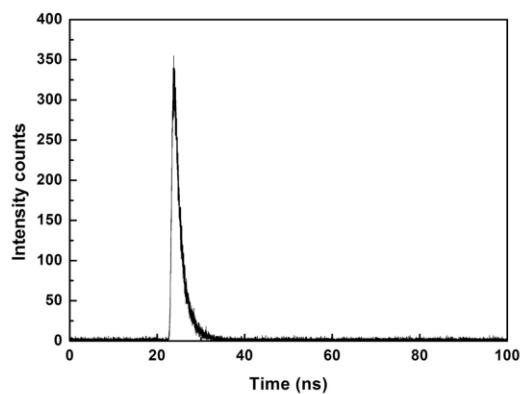
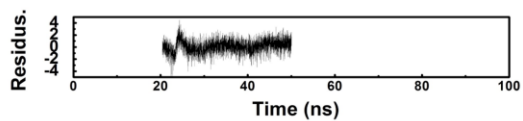
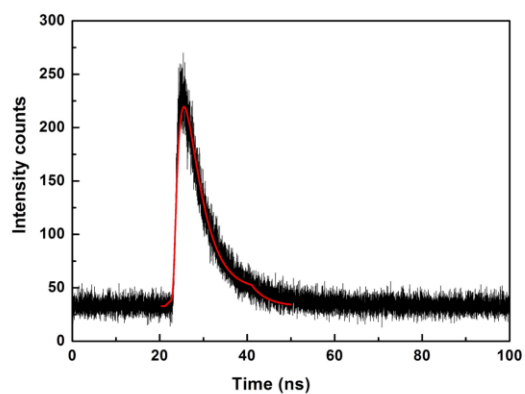


Figure S6. Tryptophan emission in the presence of dye (I) divided by the intensity of tryptophan emission in the absence of the dye (I_0). Insets, tryptophan fluorescence (λ_{ex} 280 nm) of 1 μM LmrR_W96 at increasing dye concentration from 0, red line, to 10 μM , black line.

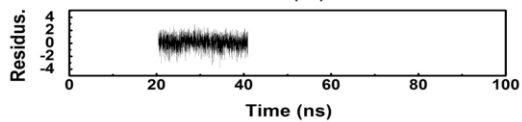
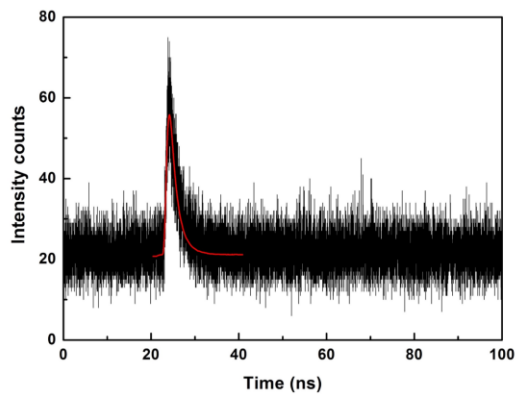
IRF (Instrument response function)



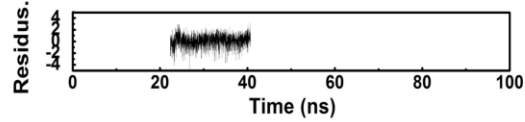
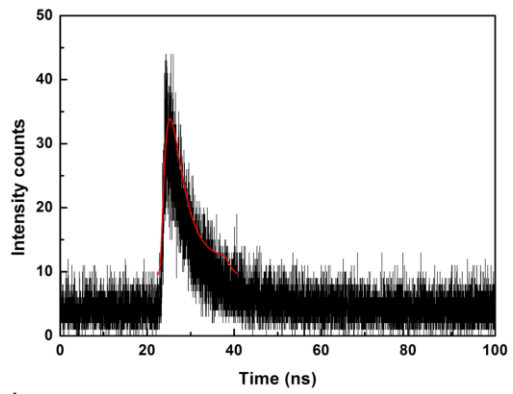
LmrR_W96



LmrR_W96+RB



LmrR_W96+PpIX



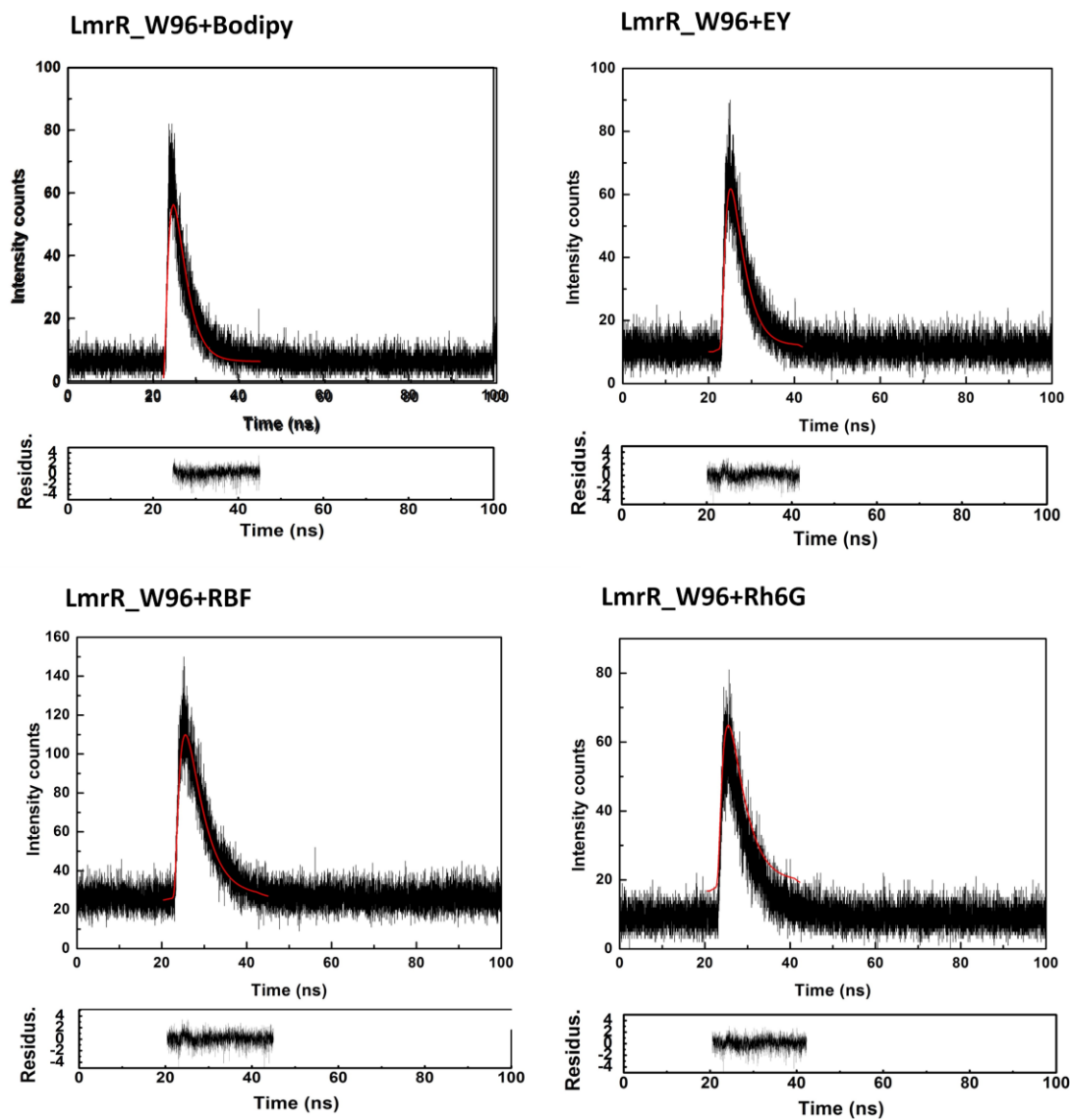


Figure S7. Tryptophan fluorescence lifetime decays for LmrR_W96 and LmrR_W96 in the presence of the dyes. Red lines indicated fit.

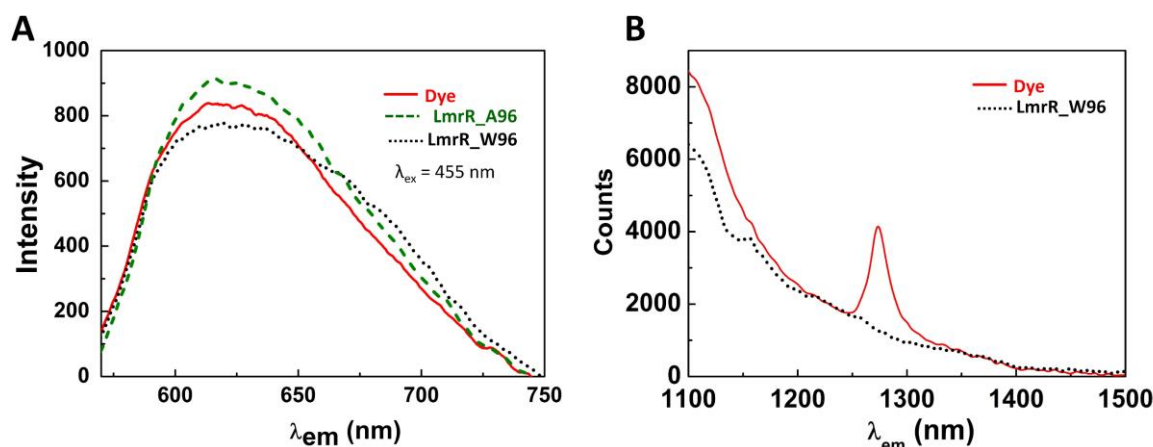


Figure S8. (a) Absorbance corrected $[\text{Ru}(\text{bpy})_3]^{2+}$ emission in phosphate buffer pD 8 (red line), in the presence of LmrR_A96 (green dashed line) and in the presence of LmrR_W96 (black dotted line). $\lambda_{\text{ex}} = 455$ nm. (b) NIR emission spectra showing $^1\text{O}_2$ phosphorescence generated by excitation of $[\text{Ru}(\text{bpy})_3]^{2+}$ ($\lambda_{\text{ex}} = 455$ nm) in D_2O (phosphate buffer pD 8) (red line) and in the presence of LmrR_W96 (black dotted line). The sloping background is due to emission from $[\text{Ru}(\text{bpy})_3]^{2+}$.

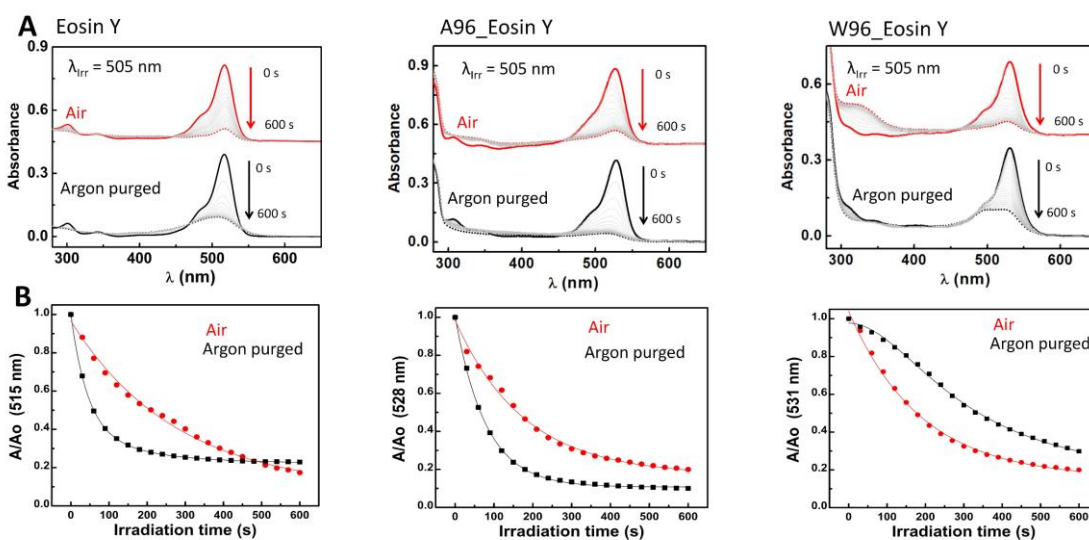


Figure S9. (a) Change in absorbance upon irradiation of eosin Y from 0 to 600 s in the presence (red) and absence (black) of O_2 (left), in the presence of LmrR_A96 (middle) and in the presence of LmrR_W96 (right). The initial spectrum (solid line); final spectrum (dashed line); grey lines are spectra recorded at 30 s intervals during continuous irradiation. (b) Absorbance with respect to initial absorbance at the maximum absorbance in the visible region of Eosin Y over time in the presence (red) and absence (black) of O_2 . Solid lines (black and red) are the fits using a model. Conditions: $4 \mu\text{M}$ eosin Y in 50 mM potassium phosphate buffer pD 8 prepared in D_2O . LmrR_A96 and LmrR_W96 are $16 \mu\text{M}$ (1:4 dye:protein ratio).

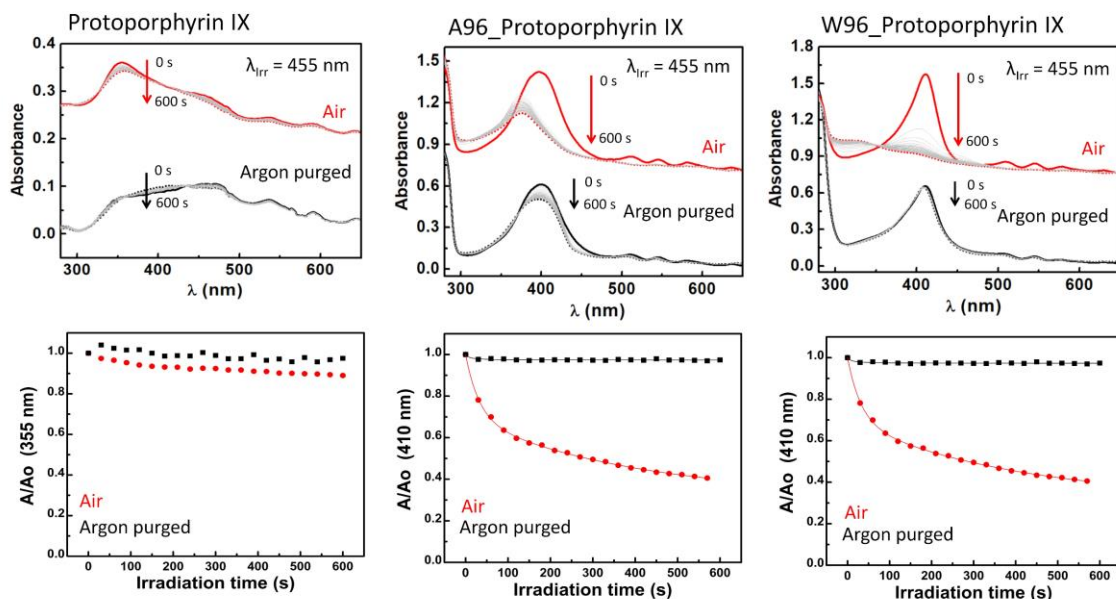


Figure S10. (a) Change in absorbance upon irradiation of protoporphyrin IX from 0 to 600 s in the presence (red) and absence (black) of O_2 (left), in the presence of LmrR_A96 (middle) and in the presence of LmrR_W96 (right). The initial spectrum (solid line); final spectrum (dashed line); grey lines are spectra recorded at 30 s intervals during continuous irradiation. (b) Absorbance with respect to initial absorbance at the maximum absorbance in the visible region of protoporphyrin IX over time in the presence (red) and absence (black) of O_2 . Solid lines (black and red) are the fits using a model. Conditions: 10 μ M protoporphyrin IX in 50 mM potassium phosphate buffer pD 8 prepared in D_2O . LmrR_A96 and LmrR_W96 are 40 μ M (1:4 dye:protein ratio).

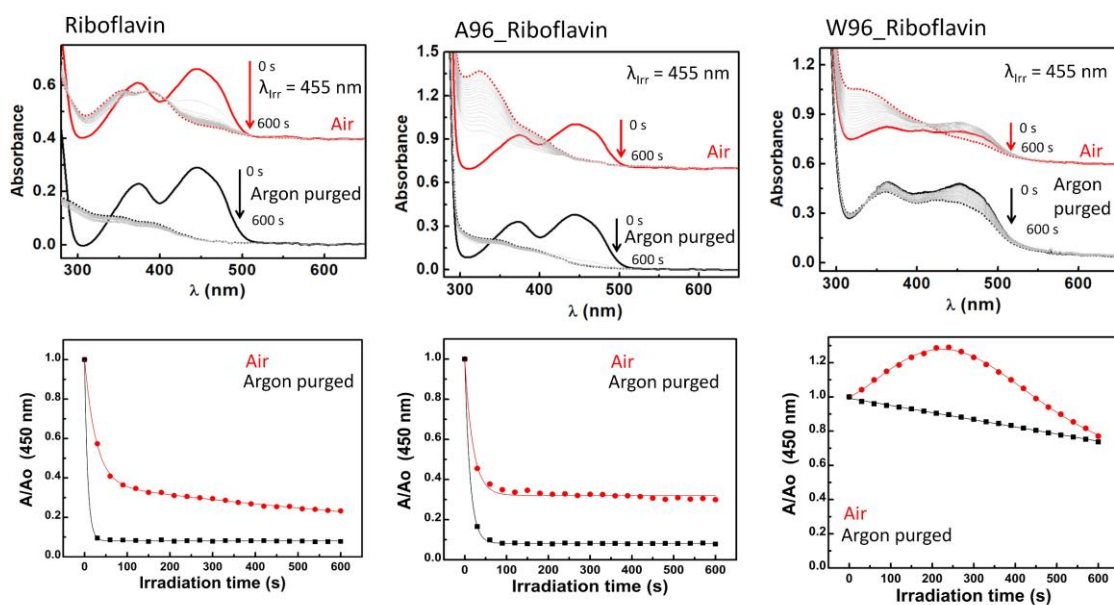


Figure S11. (a) Change in absorbance upon irradiation of riboflavin from 0 to 600 s in the presence (red) and absence (black) of O_2 (left), in the presence of LmrR_A96 (middle) and in the presence of LmrR_W96 (right). The initial spectrum (solid line); final spectrum (dashed line); grey lines are spectra recorded at 30 s intervals during continuous irradiation. (b) Absorbance with respect to initial absorbance at the maximum absorbance in the visible region of riboflavin over time in the presence

(red) and absence (black) of O₂. Solid lines (black and red) are the fits using a model. Conditions: 30 μM riboflavin in 50 mM potassium phosphate buffer pD 8 prepared in D₂O. LmrR_A96 and LmrR_W96 are 120 μM (1:4 dye:protein ratio).

Table S1. Absorbance maximum in the visible region, fluorescence maximum and Stokes shift of the dyes in solution (red), in the presence of LmrR_W96A (green) and in the presence of LmrR_W96 (black).

	Absorbance maximum in the visible region (nm)			Fluorescence maximum (nm)			Stokes shift		
	water	W96A	W96	water	W96A	W96	water	W96A	W96
Tryptophan	-	280	280	-	312	312	-	32	32
RB	549	559	563	565	573	572	16	14	9
PpIX	376	398	411	621	637	633	245	230	222
Bodipy	497	501	504	506	507	509	9	6	5
Eosin Y	515	526	531	537	538	539	22	12	8
RBF	444	444	454	526	526	526	82	82	72
Rh6G	527	527	537	551	551	551	24	24	13

Table S2. Ground state and excited state reduction (E_{red}) and oxidation (E_{ox}) potentials of dyes. E_{oo} is the energy gap between the zeroth vibrational level of the ground and excited states in the presence of LmrR_W96.

	E_{oo} (eV)	E_{red} (V vs SHE)	E_{red}^* (V vs SHE)	E_{oxi} (V vs SHE)	E_{oxi}^* (V vs SHE)
Rose bengal	2.18	-0.54	1.64	1.33	-0.85
Protoporphyrin IX	2.00	-0.23	1.77	x	x
Bodipy	2.45	-1.20	1.25	1.28	-1.17
Eosin Y	2.32	-1.06	1.26	0.78	-1.54
Riboflavin	2.49	-1.22	1.27	x	x
Rhodamine 6G	2.28	-0.71	1.57	1.63	-0.65
Tryptophan				1.09	

Table S3. Fitting of changes in visible absorbance over time under continuous irradiation for rose bengal in 50 mM phosphate buffer pD 8, in the presence of LmrR_A96 and in the presence of LmrR_W96. Models used are indicated in the table. Protein:dye ratio 1:4.

Rose bengal		
	Air	Argon purged
	$Y = A \cdot \exp(-Kx) + Y_0$	$Y = A \cdot \exp(-Kx) + Y_0$
K (s ⁻¹)	2.4×10^{-3}	2.6×10^{-3}
A	0.8	0.6
Y ₀	0.2	0.4
R-Sqr	0.99	0.99
A96_Rose bengal		
	Air	Argon purged
	$Y = A / (1 + k_1x) - K_2x + Y_0$	$Y = Y_0 - K_1x$
K ₁ (s ⁻¹)	0.9	2.8×10^{-4}
K ₂ (s ⁻¹)	2.9×10^{-4}	-
A		
Y ₀	0.8	1
R-Sqr	0.99	0.99
W96_Rose bengal		
	Air	Argon purged
	$Y = A / (1 + k_1x) - K_2x + Y_0$	$Y = Y_0 - K_1x$
K ₁ (s ⁻¹)	0.05	9.3×10^{-5}
K ₂ (s ⁻¹)	1.7×10^{-4}	-
A		
Y ₀	0.5	0.99
R-Sqr	0.99	0.99

Table S4. Fitting of changes in visible absorbance over time under continuous irradiation for bodipy in 50 mM phosphate buffer pD 8, in the presence of LmrR_A96 and in the presence of LmrR_W96. Models used are indicated in the table. Protein:dye ratio 1:4.

Bodipy	
Air	
	$Y = A \cdot \exp(-Kx) + Y_0$
K (s ⁻¹)	2.7×10^{-3}
A	1
Y ₀	0
R-Sqr	0.99
A96_Bodipy	
Air	
	$Y = A \cdot \exp(-Kx) + Y_0$
K (s ⁻¹)	2.7×10^{-3}
A	1
Y ₀	0
R-Sqr	0.99

Table S5. Protein:dye ratio 1:4. Fitting of changes in visible absorbance over time under continuous irradiation for Eosin Y in 50 mM phosphate buffer pD 8, in the presence of LmrR_A96 and in the presence of LmrR_W96. Models used are indicated in the table. Protein:dye ratio 1:4.

Eosin Y		
	Air	Argon purged
	$Y = A \cdot \exp(-Kx) + Y_0$	$Y = A \cdot \exp(-Kx) + Y_0$
K (s ⁻¹)	3.6x10 ⁻³	1.6x10 ⁻²
A	0.9	0.8
Y ₀	0.08	0.24
R-Sqr	0.99	0.99
A96_Eosin Y		
	Air	Argon purged
	$Y = A \cdot \exp(-Kx) + Y_0$	$Y = A \cdot \exp(-Kx) + Y_0$
K (s ⁻¹)	5.6x10 ⁻³	1.1x10 ⁻²
A	0.8	0.9
Y ₀	0.2	0.1
R-Sqr	0.99	0.99
W96_Eosin Y		
	Air	Argon purged
	$Y = A \cdot \exp(-Kx) + Y_0$	$Y = A / (1 + (Kx)^\beta) + Y_0$
K (s ⁻¹)	5.3x10 ⁻³	3.3x10 ⁻³
A	0.9	0.9
Y ₀	0.2	0.1
R-Sqr	0.99	0.99

Table S6. Fitting of changes in visible absorbance over time under continuous irradiation for protoporphyrin IX in 50 mM phosphate buffer pD 8, in the presence of LmrR_A96 and in the presence of LmrR_W96. Models used are indicated in the table. Protein:dye ratio 1:4.

A96_Protoporphyrin IX	
Air	
	$Y = A \cdot \exp(-Kx) + Y_0$
K (s ⁻¹)	1.8x10 ⁻³
A	0.5
Y ₀	0.5
R-Sqr	0.99
W96_protoporphyrin IX	
Air	
	$Y = A_1 \cdot \exp(-K_1x) + A_2 \cdot \exp(-K_2x) + Y_0$
K ₁ (s ⁻¹)	5.8 x10 ⁻²
K ₂ (s ⁻¹)	4.1x10 ⁻³
A ₁	0.6
A ₂	0.2
Y ₀	0.2
R-Sqr	0.99

Table S7. Protein:dye ratio 1:4. Fitting of changes in visible absorbance over time under continuous irradiation for riboflavin in 50 mM phosphate buffer pD 8, in the presence of LmrR_A96 and in the presence of LmrR_W96. Models used are indicated in the table. Protein:dye ratio 1:4.

Riboflavin		
	Air	Argon purged
	$Y = A_1 \cdot \exp(-K_1x) + A_2 \cdot \exp(-K_2x) + Y_0$	$Y = A \cdot \exp(-Kx) + Y_0$
K_1 (s ⁻¹)	3.7×10^{-2}	1.4×10^{-1}
K_2 (s ⁻¹)	8.1×10^{-4}	X
A ₁	0.6	0.9
A ₂	0.4	X
Y ₀	0	0.1
R-Sqr	0.99	0.99
A96_Riboflavin		
	Air	Argon purged
	$Y = A \cdot \exp(-Kx) + Y_0$	$Y = A \cdot \exp(-Kx) + Y_0$
K (s ⁻¹)	5.1×10^{-2}	7.9×10^{-2}
A	0.9	0.7
Y ₀	0.1	0.3
R-Sqr	0.99	0.99

Emission lifetime decay data.

Table S8. Fluorescence decay lifetime of tryptophan in the presence of quencher.

<i>Protein</i>	<i>Lifetime (ns)</i>
<i>LmrR_W96</i>	3.5
<i>LmrR_W96+PpIX</i>	2.4
<i>LmrR_W96+RB</i>	cross-correlated
<i>LmrR_W96+EY</i>	2.4
<i>LmrR_W96+Rh6G</i>	3.3
<i>LmrR_W96+RBF</i>	3.7
<i>LmrR_W96+Bodipy</i>	2.9
<i>LmrR_W96+[Ru(bpy)₃]²⁺</i>	3.1

Table S9. Fluorescence decay lifetime of dyes in solution and in the presence of LmrR_W96.

	Fluorescence lifetime (ns)
Protoporphyrin IX	
Water	cross-correlated
LmrR_W96	8.2
Methanol	14.2
DMSO	22.9
Rose Bengal	

Water	cross-correlated
LmrR_W96	cross-correlated
<i>Methanol*</i>	0.55
Acetonitrile	2.3
Eosin Y	
Water	1.12
LmrR_W96	1.8
Ethanol	3.3
DMSO	3.8
Rhodamine 6G	
water	4.1
LmrR_W96	3.8
DMSO	3.8
Riboflavin	
Water	4.5
LmrR_W96	4.5
Acetonitrile	4.7
Bodipy	
Water	1.7
LmrR_W96	4.7
Methanol	3.7

*D. Huppert, S. D. Rand, A.H. Reynolds and P.M. Rentzepis, *J. Chem. Phys.* **1982**, 77, 1214-1224